ELSEVIER

Polymer 42 (2001) 6009–6018

polymer

www.elsevier.nl/locate/polymer

Off-line monitoring of butyl acrylate, methyl methacrylate and vinyl acetate homo- and copolymerizations in toluene using ATR-FTIR spectroscopy

Hong Hua, Marc A. Dubé*

Department of Chemical Engineering, University of Ottawa, 161 Louis Pasteur Street, P.O. Box 450, Stn. A, Ottawa, Ont., Canada K1N 6N5

Received 12 September 2000; received in revised form 16 January 2001; accepted 17 January 2001

Abstract

Butyl acrylate, methyl methacrylate, and vinyl acetate solution homo- and copolymerizations were monitored using ATR-FTIR spectroscopy with conduit and diamond-composite sensor technology. Monomer conversion and copolymer composition changes as a function of time were calculated by monitoring the peak height of characteristic absorbances of monomers. Results obtained from the ReactIR™ 1000 reaction analysis system agreed well with those determined by traditional gravimetry and ^{1}H-NMR spectroscopy. Improved models developed previously to incorporate solvent effects on solution polymerizations of butyl acrylate and vinyl acetate monomers were applied to predict monomer conversion, copolymer composition and molecular weight averages. Comparisons between experimental data and model predictions are presented in this study.

Keywords: Butyl acrylate; Methyl methacrylate; Vinyl acetate

1. Introduction

As the polymer industry becomes more competitive, polymer manufacturers face increasing pressures for production cost reductions and more stringent polymer quality requirements [1]. Therefore, the development of comprehensive methods to control polymer quality (in terms of polymer reactor operation and polymer property trajectory monitoring) during a polymerization is key to the efficient production of tailored, high quality polymers and the improvement of plant operability and economics.

Traditional polymerization monitoring is carried out by sampling and off-line characterization of polymer quality that is done in a laboratory on discrete samples taken from a process flow line. For example: gravimetry and gas chromatography (GC) are used to measure monomer conversion; nuclear magnetic resonance (NMR) spectroscopy can be used to obtain cumulative composition, sequence length, and other structural information about the polymer produced in multicomponent polymerizations; and gel permeation chromatography (GPC) is used with a variety of detectors to obtain molecular weight information of the produced polymers.

Nowadays, the increasing demand for the production of polymers of high quality with prespecified properties places more emphasis on the development of accurate and robust analytical instrumentation and sensors for the on-line monitoring of polymerization reactions. Many of the problems encountered in polymerization reactor control can be attributed to the lack of on-line measurements of the reaction evolution [2]. For polymer reactions, on-line monitoring devices adapted to industrial processes must have satisfactory analysis and response time behaviour to be able to measure continuously. In addition, they have to supply correct results over long periods of time in environments inherent to polymer reaction processes that are often physically and chemically aggressive. Different techniques now available can be classified as direct and indirect. The former methods involve monitoring of the residual monomer content in the reactor, while the latter methods measure a property change of the polymerization system that can be related to the mass of monomer or formed polymer. The term *on-line* mentioned here refers to a device for analysis that is connected to the process stream via a side-loop or sample thief while the term *in-line* refers to a device that obtains the measurement directly in the process stream [3].

To improve the quality of the control of polymer properties such as copolymer composition, one must be able to follow the advancement of a polymerization reaction first,

* Corresponding author. Tel.: +1-613-562-5800; fax: +1-613-562-5172.
E-mail address: dube@genie.uottawa.ca (M.A. Dubé).

0032-3861/01/$ - see front matter
PII: S0032-3861(01)00085-4

i.e. follow key measurements such as the individual monomer conversions and polymer composition during the process. By using the on-line sensed information, the task to control the system parameters and guide the process along an optimum path can be successfully accomplished. Thus, real-time monitoring of the polymerization reaction is of crucial importance in efforts to optimize polymerization processes and polymer product qualities.

Among various densimetry, calorimetry, GC and spectroscopy monitoring techniques, mid-infrared (MIR) spectroscopy has significant potential. Compared to near infrared (NIR), the MIR range, extending from 4000 to 400 cm^{-1}, is the preferred choice owing to the unmatched wealth of molecular level information contained in the infrared portion of the electromagnetic spectrum [4]. In-situ Fourier transform infrared (FTIR) spectroscopy is a state-of-the-art monitoring technique that is well suited to obtain real-time structural and kinetic information on a polymerization process. In addition, when using FTIR, reactions can be analyzed without expensive reactor modifications, complicated sampling methods, and difficult experimental operations.

Mijovic et al. [5] described an inexpensive remote MIR–FTIR spectroscopy set-up utilizing gold-coated hollow waveguides instead of fibre optics to investigate the cure of a multifunctional epoxy/amine formulation. They monitored the change of characteristic absorption band intensities. The evaluated reaction kinetic data agreed with the data from NIR spectroscopy in the range extending from 14,000 to 4000 cm^{-1}, up to about 60% conversion. Doyle [6] described an MIR–FTIR spectroscopy set-up to investigate free radical copolymerization of styrene and methyl methacrylate (MMA) in toluene on-line. An attenuated total reflection (ATR) immersion probe was designed and connected with an FTIR instrument through metallic hollow waveguides. The toluene spectrum was easily subtracted from the spectra of the reaction mixture. A convenient set of spectral bands for both monomers was selected for quantitative analysis using a computer program to solve simultaneous equations for estimating individual monomer conversions. The probe was shown to yield an intimate view of a polymerization reaction with continuous on-line data, making it possible to optimize its parameters and to terminate the reaction at any desired degree of completion. Puskas et al. [7,8] described an example of in-situ monitoring of cationic polymerization of isobutylene and styrene by using a fibre optic ATR probe in conjunction with an FTIR instrument in the MIR region. The results compared favourably with a developed kinetic model. Storey et al. [9–11] have reported their use of a ReactIR™ 1000 reaction analysis system (ASI Applied Systems, Metter-Toledo Corp.) equipped with a light conduit and DiComp (diamond-composite) insertion probe. Their efforts focused on the development of a method for experimentally determining kinetics of the cationic polymerization of isobutylene through in-situ, real-time reaction monitoring by utilizing MIR–FTIR spectroscopy. Pasquale et al. [12] also used the same instrument to study the kinetics of stable free radical polymerizations of styrene.

Butyl acrylate/methyl methacrylate/vinyl acetate (BA/MMA/VAc) terpolymers, and their corresponding homo- and copolymers are commercially important components in many paints, adhesives, and binders. Dubé and Penlidis [13–15] described in detail a systematic approach to the study of multicomponent batch polymerization kinetics of this system in bulk, solution, and emulsion. All the analyses were done off-line. Gravimetric analysis of monomer consumption was used to estimate conversion, proton nuclear magnetic resonance (^{1}H-NMR) spectroscopy was used to measure the polymer composition and GPC was used to measure molecular weight averages. Due to the widely differing monomer reactivity ratios in the batch polymerizations containing VAc, polymer composition drift was significant during the process. The acrylic monomer was preferentially consumed during the early stages of the reaction resulting in copolymers containing only small amounts of VAc at the beginning of the reaction. As the reaction proceeded, the acrylic monomer was completely depleted and the remaining unreacted VAc monomer was polymerized. Thus, the final product contained polymers with a distribution of compositions and microstructures. In order to produce polymers with homogeneous properties, semi-batch policies to control the monomer feed coupled with on-line monitoring based on analysis of the overall monomer concentrations are often used [16]. However, traditional off-line methods are unable to monitor the polymerization in an adequate time frame when violent composition drifts occur during the process. Some current sensing techniques such as on-line GC also pose sampling difficulties [17].

In this paper, we report the results of a solution homopolymerization of MMA and solution copolymerizations of BA/MMA and MMA/VAc initiated with 2,2′-azobisisobutyronitrile (AIBN), and conducted in toluene (50 wt%) at 60°C. The ReactIR™ 1000 reaction analysis system was used for off-line analysis of our samples to identify characteristic peaks, to follow the reaction kinetics and to evaluate its ability to estimate monomer conversion and polymer composition from spectral changes. These off-line experiments were a necessary precursor to future in-line polymerization monitoring studies. Kinetic data obtained through IR analysis were compared to results from the traditional gravimetric and ^{1}H-NMR methods. Results were also compared to predictions from a mechanistic model.

2. Experimental section

2.1. Materials

Purification of reagents was performed by classical

methods [13]. The monomers BA and MMA (Aldrich Chemical Co. Inc.) were washed three times with a 10% sodium hydroxide solution to remove the inhibitor and subsequently washed three times with distilled water. Calcium chloride ($CaCl_2$) was added to remove any residual water. These monomers were freshly distilled under vacuum at the most 24 h before use. The monomer VAc (Aldrich Chemical Co. Inc.) was also distilled under vacuum at the most 24 h before use. The first 20–50 ml of distillate were discarded (distillate bottoms). All purified monomers were stored at −10°C when not in use. The initiator 2,2′-AIBN (Polysciences Inc.) was recrystallized three times from absolute methanol. The chain transfer agent (CTA) 1-dodecanethiol (Acros Organics) was used as received. All of the solvents used in these experiments and for characterization of the copolymers (toluene, ethanol, deuterated chloroform, tetrahydrofuran (THF)) were also used as packaged.

2.2. Instrumentation

A ReactIR™ 1000 reaction analysis system equipped with a light conduit and DiComp (diamond composite) insertion probe was used to collect mid-FTIR spectra of the polymerization components. These spectra were used to calculate monomer conversion and, for the case of copolymerization, polymer composition. Resulting polymer compositions were also obtained through ^{1}H-NMR spectra taken by a Bruker AMX500 Fourier-transform ^{1}H-NMR spectrometer. Polymer molecular-weight averages and molecular-weight distributions were determined with a Waters Associates GPC system equipped with three Waters Styragel-HR columns (10^3, 10^4, and 10^6 Å pore size) installed in series, thermostated to 30°C, and a Waters 410 differential refractometer thermostated to 38°C. THF was used as the mobile phase and was delivered at 0.3 ml/min.

2.3. Procedures

High conversion solution polymerizations of MMA homopolymer and two copolymer pairs, BA/MMA and MMA/VAc, were run at 60°C in a 50 wt% toluene solution. Further details of the reaction conditions are shown in Table 1.

Polymerizations were carried out in glass ampoules of length 20 cm and outer diameter 0.8 cm. The monomers and initiators, together with solvent and CTA, were weighed into a flask to prepare the initial feed and an amount of about 2.7 ml was then pipetted into several numbered ampoules. Next, the ampoules were degassed through several vacuum freeze–thaw cycles and subsequently submerged in a water bath for a recorded time interval with the temperature controlled at 60°C. Two ampoules were taken out at the same time, one for traditional polymer analysis and the other for IR spectroscopy analysis, and submerged in liquid nitrogen to quench the reaction.

Table 1
Reaction conditions (all monomer values in mole fraction)

Ingredient	M1	BM1	BM2	MV1	MV2	MV3	MV4
BA	–	0.5	0.4	–	–	–	–
MMA	1.0	0.5	0.6	0.5	0.4	0.5	0.4
Vac	–	–	–	0.5	0.6	0.5	0.6
AIBN (mol/l)	0.05	0.1	0.1	0.05	0.05	0.1	0.1
CTA (mol/l)	0.05	0.025	0.025	0.025	0.05	0.025	0.025

For the traditional analysis, the content of one ampoule was poured into a 10-fold excess of ethanol. Mass conversion based on the total polymer in the reaction mixture was measured using gravimetry. In the case of copolymers, the resulting isolated polymers were analyzed for cumulative polymer composition by ^{1}H-NMR spectroscopy. Analysis was carried out at room temperature in deuterated chloroform (~2% (w/v) solutions), which was used both as the solvent and the reference. Acquisition time was 4.6 s, and 16 scans were performed per readout (for averaging). The relative amounts of monomer bound in the copolymer were estimated from the areas under the appropriate absorption peaks of the spectra. All spectra exhibited good peak separations for a straightforward interpretation of the results. For BA/MMA copolymers, the spectral peaks for the $-OCH_2$ group in BA were located at ~4.0 ppm and those for the $-OCH_3$ group in MMA were at ~3.6 ppm. The MMA/VAc copolymers exhibited peaks for the α-hydrogen in VAc at ~4.9 ppm and the $-OCH_3$ group in MMA at ~3.6 ppm. The individual conversion profile for each monomer was obtained by combining results from the overall conversions through gravimetry and each monomer's corresponding mole fraction in the copolymer chain through ^{1}H-NMR spectroscopy.

The resulting polymer molecular-weight averages and molecular-weight distributions were determined by GPC. THF (HPLC grade) was used as the carrier fluid and reference. Polymer samples were dissolved in THF to produce solutions with a concentration of 0.001–0.002 g/10 ml and filtered through 0.45 μm filters to remove any high molecular weight gel. 200 μl of each solution was injected into the GPC and the data were analyzed using the Millennium 32™ (version 3.05) chromatography manager software. Polymer molecular weights were calculated using the universal calibration principle, given the Mark–Houwink, K and α, parameters of polymers in THF (polystyrene, $K = 1.6 \times 10^{-2}$ ml/g, $\alpha = 0.700$ [18]; polybutyl acrylate, $K = 1.1 \times 10^{-2}$ ml/g, $\alpha = 0.708$ [19]; polymethyl methacrylate, $K = 1.28 \times 10^{-2}$ ml/g, $\alpha = 0.690$ [18]; polyvinyl acetate, $K = 1.56 \times 10^{-2}$ ml/g, $\alpha = 0.708$ [20]). K and α values for the copolymers were obtained using weighted averages based on the cumulative copolymer composition data.

The contents in each duplicate ampoule were poured into 5-dram vials and were analyzed using the ATR-FTIR insertion probe. The standard acquisition mode of the ReactIR™

1000 was used to collect the IR spectra. The ATR-FTIR data were comprised of spectra collected from 64, 128, and 1024 scans, over the spectral ranges of 4000–700 cm^{-1}, with either 4 or 8 cm^{-1} resolution. At 4 cm^{-1} resolution, the spectral acquisition times associated with those numbers of scans were approximately 21.3, 42.7, and 341.3 s, respectively. The insertion probe was put into the vial to record the spectra of the polymerization contents. The spectra were recorded and further analyzed using the ReactIR™ (version 2.2) software.

Monomer conversion monitoring was accomplished by following the change of certain characteristic peaks in the MIR spectra during the polymerization process. It was assumed that the component concentrations were proportional to absorbances measured as the corresponding peak heights. Eqs. 1 and 2, reported by Chatzi et al. [21], were used to calculate the conversion, x, of individual monomers:

$$x(\text{mol\%}) = 1 - \frac{\text{peak height at time } t}{\text{peak height at time } t = 0} \quad (1)$$

and the overall conversion, X, of the copolymerization:

$$X(\text{wt\%}) = \frac{w_i}{w_i + w_j} x_i(\text{mol\%}) + \frac{w_j}{w_i + w_j} x_j(\text{mol\%}), \quad (2)$$

where $w_i/(w_i + w_j)$ was the weight fraction of monomers i fed into the reactor at time $t = 0$.

Typically, a resolution of 4–8 cm^{-1} is adequate for good peak resolution and high signal to noise ratio for most condensed phase samples such as polymer solutions. Using a higher resolution would give noisier spectra and extend the data acquisition time, while there would be no improvement in peak assignment and measurement accuracy compared to the lower resolution spectra [22]. If reaction kinetics are fast, the number of scans should be kept low in order to capture the reaction process. However, more scans would give spectra with a higher signal-to-noise ratio.

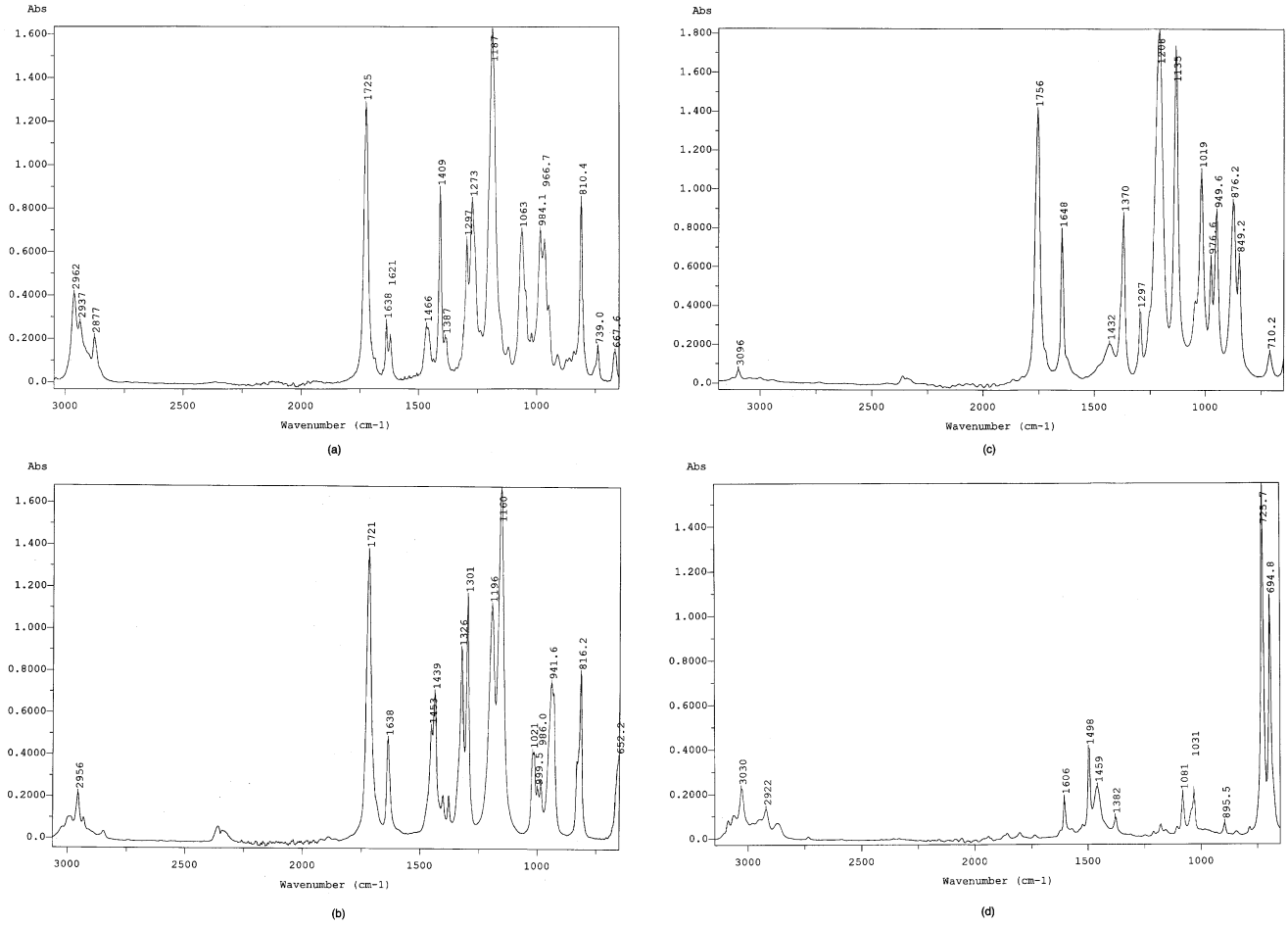

Fig. 1. (a) ATR-FTIR spectrum of butyl acrylate monomer. (b) ATR-FTIR spectrum of methyl methacrylate monomer. (c) ATR-FTIR spectrum of vinyl acetate monomer. (d) ATR-FTIR spectrum of toluene.

3. Results and discussion

3.1. Data acquisition

An FTIR spectrum of a solution polymerization will include absorbances of monomer, produced polymer, and solvent. The solvent absorbance may interfere with the quantitative analysis of monomer and polymer absorbances if it overlaps with them. One way to solve the problem is to subtract the solvent spectrum to show the pure component spectrum of the reaction mixture using the data manipulation software. However, few subtractions yield a clear spectrum with a flat baseline and no solvent bands [22].

An alternative can be to choose a region without solvent absorbance interference for quantitative analysis, thus rendering the spectral subtraction unnecessary. Toluene was used as the solvent in our solution polymerizations. It exhibited strong absorbances at 1606, 1498, and 1459 cm^{-1} for benzene ring stretching; 1081 and 1031 cm^{-1} for aryl CH bending; and 896, 726, and 695 cm^{-1} for aryl CH wagging. Thus, those wavenumbers were avoided when choosing characteristic absorbances for quantitative analysis of the monomers.

The successful use of an in-line spectroscopic sensor for monitoring polymerization, especially for copolymerization reactions, also presupposes the existence of characteristic absorbance bands for monomers and the individual structural units in the polymer. The characteristic group frequencies will generally appear in the same region for polymers as for monomers, which may also interfere with analysis on monomer bands. While specific couplings can occur with regularly ordered chemical functional groups in polymers, these couplings shift the group frequencies so that those bands can be distinguished from those of the monomers in the spectra. For copolymerization cases, absorbance bands from different monomers chosen for quantitative analysis should not overlap with each other.

Figs. 1a–d show the spectra of pure BA, MMA, VAc and toluene. Based on the heuristics mentioned above, 1409 cm^{-1} of CH deformation for BA, 1326 cm^{-1} of C–O–C stretching for MMA, and 876 cm^{-1} of $=CH_2$ wagging for VAc were found to be suitable to follow the copolymerizations.

3.2. MMA homopolymerization

One MMA homopolymerization run was conducted in 50 wt% toluene solution (see Table 1). Fig. 2 shows the distinct reaction mixture spectral changes as the consequence of the polymerization reaction. Characteristic absorbance bands for monomer were easily identified such as the C=C stretching at 1640 cm^{-1}, the C–O–C stretching vibration of the aliphatic ester group at 1324 cm^{-1}, and the C=O wag at 652 cm^{-1} (see also Fig. 1b), which all diminished with increasing reaction time. Those peaks did not overlap with the peaks from the polymer produced nor from those due to the solvent. Thus, no solvent subtraction was required for the analysis of the overall spectra. A quantitative estimate of the monomer conversion during the reaction was made by calculating the ratio of the absorbances of the 1640, 1324, and 652 cm^{-1} characteristic absorption bands at reaction time t to each of their corresponding peaks at the start of the polymerization reaction ($t = 0$), according to Eq. (1). The absorbance of each peak was measured as the peak height referenced to a single-point baseline after baseline correction. The absorbance at the start of the reaction was the absorbance of the reaction contents measured prior to polymerization.

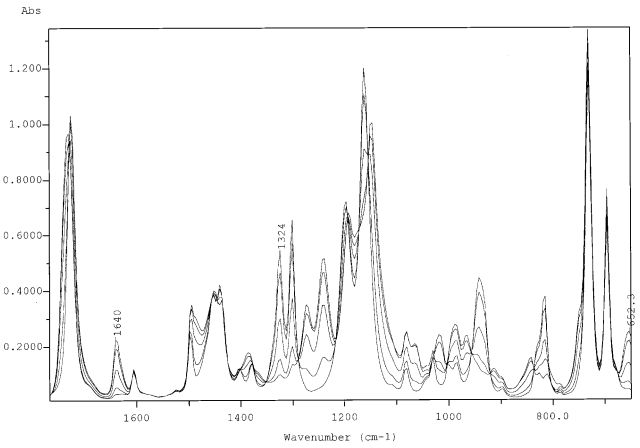

Fig. 2. ATR-FTIR spectra of MMA solution polymerization run M1 in toluene (50 wt%).

The monomer conversion estimated from the ATR-FTIR spectra agreed with the conversion values obtained from conventional gravimetric measurements, as shown in Fig. 3. It is evident that any of these characteristic absorbance bands (i.e. 1640, 1324, and 652 cm^{-1}) can be used for real-time monitoring of MMA homopolymerization.

The monomer conversion data of the polymerization from gravimetric and IR spectral methods were also

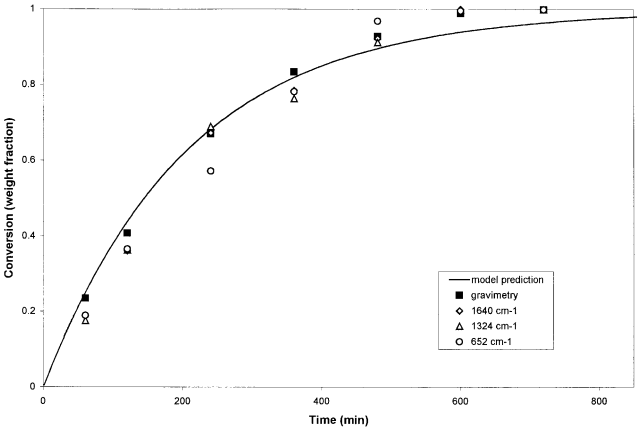

Fig. 3. MMA homopolymerization run M1: conversion vs. time.

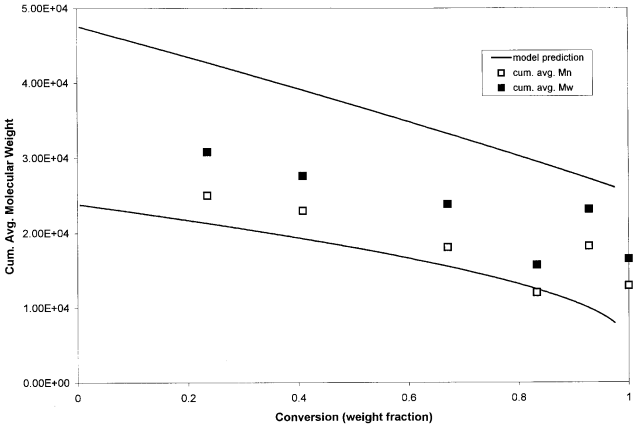

Fig. 4. MMA homopolymerization run M1: cumulative number- and weight-average molecular weight vs. conversion.

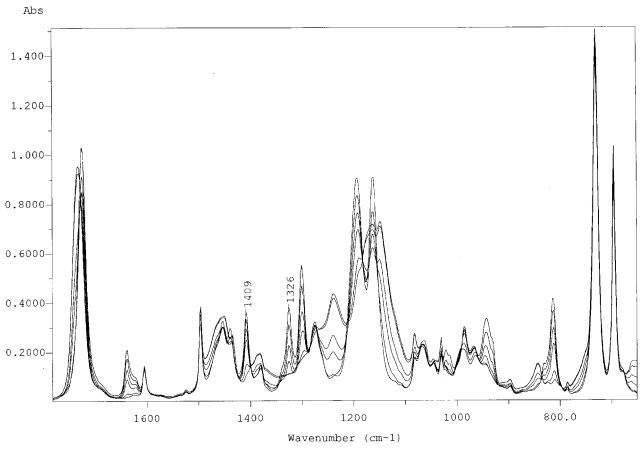

Fig. 5. ATR-FTIR spectra of BA/MMA solution copolymerization run BM2 in toluene (50 wt%).

compared to predictions from a JAVA™-based computer simulation [23] in Fig. 3. This computer simulation was developed using the mathematical model described by Dubé et al. [24]. The model has been validated for a wide range of homopolymerization and copolymerization systems including BA, MMA, and VAc by Gao and Penlidis [25,26]. Model predictions appear to be reasonable in this case.

The kinetics of the homopolymerization of MMA have been studied extensively and are well understood. However, the issue of solvent effects on the propagation and/or termination rate constants is of concern. Fernandez-Garcia et al. [27] showed that the propagation rate constant for MMA polymerized in toluene was not significantly different from that in bulk polymerization, while the termination rate constant was dependent on the polymer chain length. Coote et al. [28] also concluded that solvent effects were small for MMA solution homopolymerization. Thus, the good predictions of our model without modification for solvent effects are supported by these recent publications. Nonetheless, the model correctly captures the effect of the solvent on the reduction of the viscosity of the reaction mixture and the resulting decrease in the polymerization rate. This decrease in rate is because the lower viscosity permits easier diffusion of the polymer chains and thus, a higher rate of termination.

The change of the cumulative number- and weight-average molecular weights with conversion was plotted as shown in Fig. 4, and compared to model predictions. The products exhibited narrower molecular weight distributions than those predicted by the model. These differences are probably due to uncertainty in the chain transfer to CTA rate parameters for MMA.

3.3. BA/MMA copolymerization

Two BA/MMA copolymerization runs were conducted in a 50 wt% toluene solution (see Table 1). Reaction mixture spectra were collected in the same way as for the MMA homopolymerization and distinct changes as the consequence of the polymerization reaction were observed (see Fig. 5). Characteristic absorbance bands for both monomers were easily identified at 1409 cm^{-1} for the BA hyperconjugated =CH deformation (see also Fig. 1a) and at 1326 cm^{-1} for the MMA C–O–C stretching vibration of the aliphatic ester group (see also Fig. 1b), which diminished with increasing reaction time. There was neither interference from the polymer nor from the solvent absorbances around these regions. Thus, these two peaks were used for tracking the reaction. The 1640 cm^{-1} C=C stretching and 652 cm^{-1} C=O wagging for MMA were not used because they overlapped with BA's 1638 cm^{-1} C=C doublet and 668 cm^{-1} C=O wagging, which could introduce error into the profile for MMA concentration over time.

A quantitative estimate of the individual conversion of both monomers during the reaction was made by calculating the ratio of the absorbances (peak height referenced to a single-point baseline after baseline correction) of the 1409 and 1326 cm^{-1} characteristic absorption bands, for BA and MMA, respectively, at reaction time t to those corresponding peaks at the start of the polymerization reaction ($t = 0$), according to Eq. 1. The absorbances at the start of the reaction were the absorbances of the reaction contents measured prior to polymerization. The overall weight percentage conversion was subsequently calculated according to Eq. 2. Figs. 6 and 7 show good agreement of the overall and individual monomer conversion data obtained between traditional gravimetry and ^{1}H-NMR spectroscopy techniques and ATR-FTIR spectroscopy.

From Figs. 6 and 7, a slightly higher overall copolymerization rate was observed when the MMA mole fraction in the feed was increased from 0.5 to 0.6. Because of the reactivity ratios for the BA/MMA pair ($r_{BA} = 0.291$ and

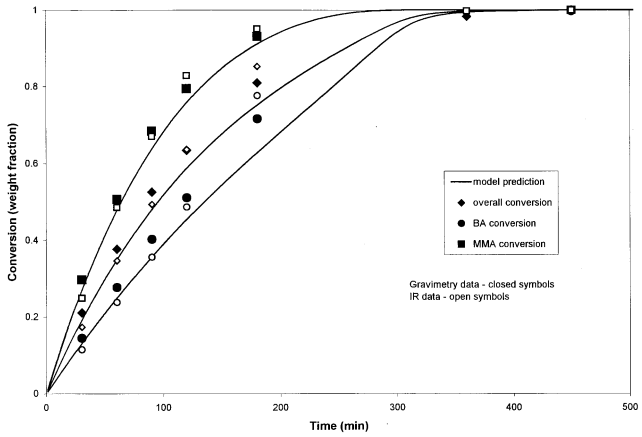

Fig. 6. BA/MMA solution copolymerization run BM1: conversion vs. time.

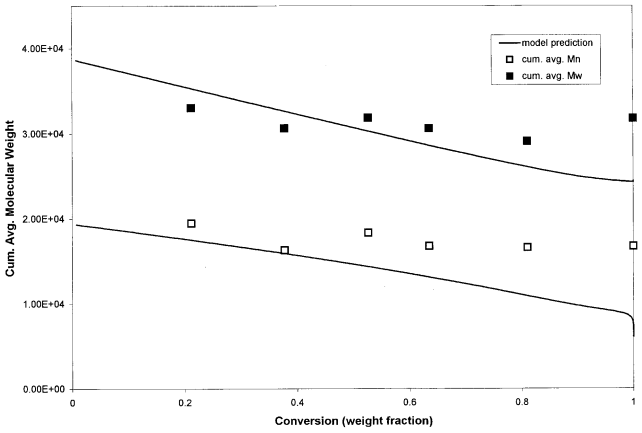

Fig. 8. BA/MMA solution copolymerization run BM1: cumulative number- and weight-average molecular weight vs. conversion.

$r_{MMA} = 1.871$) 29], MMA was slightly more rapidly consumed when copolymerized with BA such that only a minor composition drift could be observed during the polymerization.

As an example, the cumulative number- and weight-average molecular weights of the produced copolymers were plotted for run BM1 and are shown in Fig. 8. The use of CTA in the solution polymerizations helped keep the copolymer molecular weights low and the molecular weight distribution narrow and unchanged during the process.

There have been only limited kinetic studies for the BA/MMA solution copolymerization. Hakim et al. [30] studied solvent effects on the BA/MMA reactivity ratios in toluene over an extended temperature range from 60 to 140°C. No significant solvent effects on copolymer composition were detected. Madruga et al. [31] reported on the homo- and copolymerization of BA/MMA in benzene solution. They found that the lumped parameter, $k_p/k_t^{0.5}$ (where k_p is the propagation rate constant and k_t is the termination rate constant), for the BA homopolymerization, decreased when the monomer concentration in the solution decreased while it did not change in the case of MMA. McKenna et al. [19] demonstrated similar phenomena for BA polymerizations in toluene. In solution polymerizations, the higher solvent concentration will increase the number of chain transfer to solvent reactions to create more short-chain radicals and thus, decrease the viscosity of the reaction mixture. This will in turn, increase the termination rate parameter and decrease the value of the lumped parameter. This is because short radicals move and terminate more quickly in less viscous environments. At the same time, the toluene solvent reduces the viscosity of the reaction mixture by dilution. The associated decrease in polymerization rate follows.

Thus, model parameters for BA were modified according to Jovanovic and Dubé [32] who modelled the BA/VAc in toluene solution copolymerization. Model predictions of conversion, composition and molecular weight averages are in agreement with the collected data (see Figs. 6–8). For the prediction of the BA/MMA solution copolymerizations, homopolymerization parameters for BA and MMA in toluene were used. There is uncertainty in some of the parameters related to the molecular weight development (e.g. chain transfer to CTA and chain transfer to polymer rate parameters). With future improvements to these parameters, improved model predictions should follow.

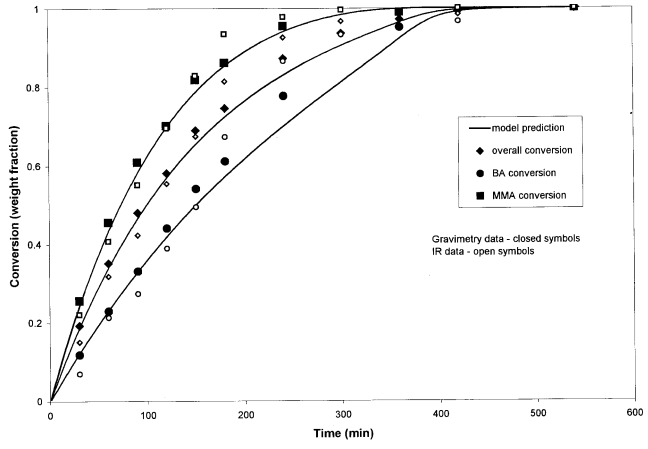

Fig. 7. BA/MMA solution copolymerization run BM2: conversion vs. time.

3.4. MMA/VAc copolymerization

Four MMA/VAc copolymerization runs were conducted in a 50 wt% toluene solution (see Table 1). Reaction mixture spectra were collected the same way as for the other polymerization runs and distinct changes as the consequence of the polymerization reaction were observed (see Fig. 9). Characteristic absorbance bands for both

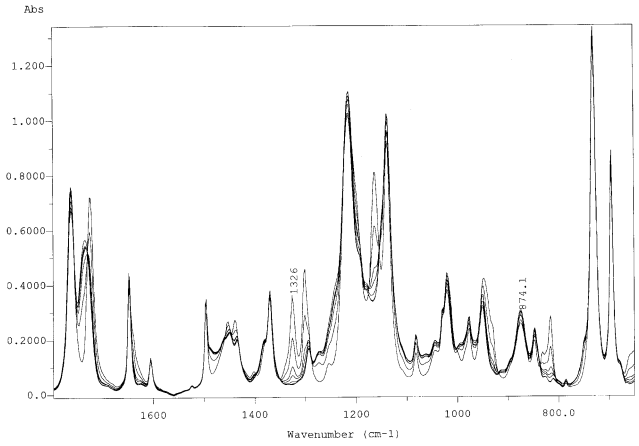

Fig. 9. ATR-FTIR spectra of MMA/VAc solution copolymerization run MV3 in toluene (50 wt%).

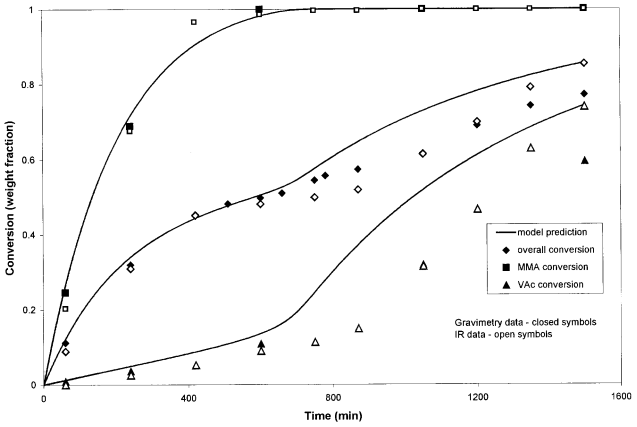

Fig. 11. MMA/VAc solution copolymerization run MV2: conversion vs. time.

monomers were identified at 1326 cm^{-1} for the MMA C–O–C stretching vibration of the aliphatic ester group (see also Fig. 1b) and at 874 cm^{-1} for the VAc $=CH_2$ wagging (see also Fig. 1c), which diminished with increasing reaction time. There was no interference from the polymer or from the solvent absorbances around these regions. Thus, these two peaks were used for tracking the reaction. Since the 1640 cm^{-1} C=C stretching for MMA overlapped somewhat with VAc's 1648 cm^{-1} C=C stretching, they were not used for the profiles of either monomer's concentration over time.

The individual conversions of both MMA and VAc monomers during the reactions were estimated similar to that for the BA/MMA copolymerizations. The overall weight percentage conversion was subsequently calculated according to Eq. (2). The monomer conversion vs. time data obtained from the different measurement techniques are plotted as shown in Figs. 10–13. Good agreement was observed for MMA between the ATR-FTIR measurements and the measurements from the gravimetric and ^{1}H-NMR techniques for both the overall and the individual monomer conversions.

Final conversions ranging from 60 to 80 wt% were achieved in the experiments. They all exhibited a two-stage rate effect as described in Dubé and Penlidis [13]. Since MMA is much more reactive than VAc according to the reactivity ratios ($r_{MMA} = 24.025$ and $r_{VAc} = 0.0261$) [33], MMA dominated the beginning of the reaction to form polymer mostly composed of MMA while VAc dominated the polymerization after the MMA was depleted. As shown in Figs. 10–14, VAc was not reacting much during the early stages of the copolymerizations and behaved much like a solvent so that the MMA homopolymerization gel effect was dampened by the VAc. During the latter stages of reaction, the polymerization rate was very high, owing to the fact that the VAc homopolymerization exhibited an autoacceleration in the high viscosity environment of the polymer chains. Comparison between Figs. 10 and 11, and Figs. 12 and 13 indicate that when the MMA mole fraction in the monomer feed was increased from 0.4 to 0.5, the

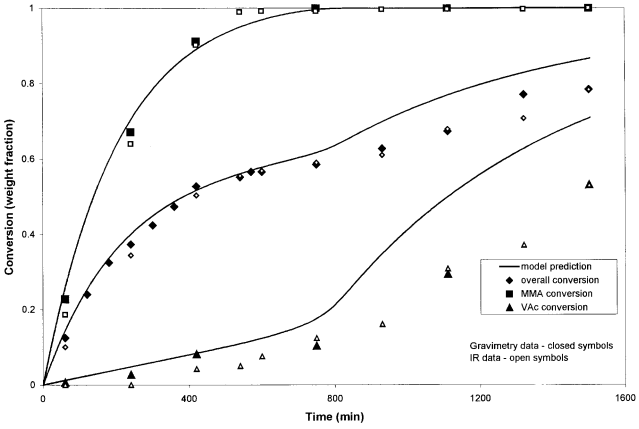

Fig. 10. MMA/VAc solution copolymerization run MV1: conversion vs. time.

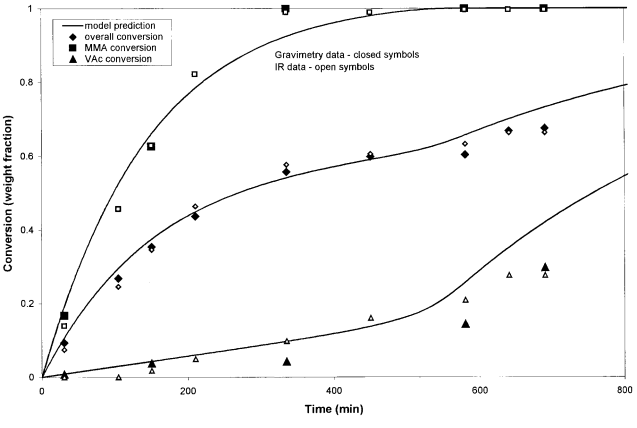

Fig. 12. MMA/VAc solution copolymerization run MV3: conversion vs. time.

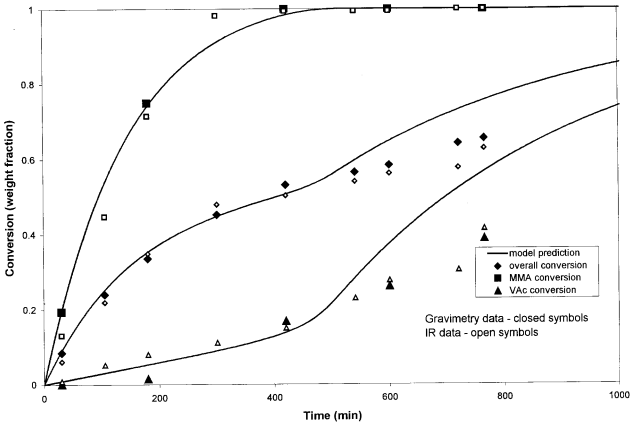

Fig. 13. MMA/VAc solution copolymerization run MV4: conversion vs. time.

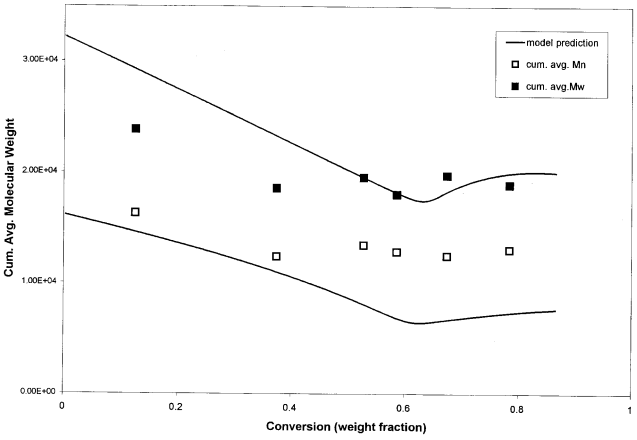

Fig. 15. MMA/VAc solution copolymerization run MV1: cumulative number- and weight-average molecular weight vs. conversion.

two-stage rate effect was delayed to higher conversions. Higher polymerization rates were also observed during the first stage of the polymerization while the overall polymerization rates did not change very much. The increase in initiator concentration from 0.05 to 0.1 mol/l, as shown in Figs. 10 and 12, and Figs. 11 and 13 also increased the overall rates of polymerization according to classical kinetic theory. On the other hand, the toluene solvent reduced the viscosity of the reaction mixture and consequently, the rate of polymerization.

Cumulative copolymer compositions were plotted as a function of conversion and are shown for runs MV1 and MV2 in Fig. 14 as an example. Significant copolymer drift was observed at higher conversion levels (above 50%). This coincided with the two-stage rate effect shown in Figs. 10 and 11. Furthermore, when the MMA fraction in the monomer feed was increased, the two-stage rate effect was delayed to higher conversions. Comparing BA/MMA and MMA/VAc runs using the same initiator and CTA concentration conditions, striking differences can be seen. Due to the difference in the reactivity ratios for BA/MMA as compared to MMA/VAc, the latter exhibited a much larger composition drift.

As an example, the cumulative number- and weight-average molecular weights vs. conversion data, together with model predictions for runs MV1 and MV2 were plotted and are shown in Figs. 15 and 16. Similar plots were obtained for runs MV3 and MV4 (not shown). As shown in Figs. 15 and 16, a higher MMA fraction in the monomer feed resulted in slightly faster polymerization rates and thus, higher molecular weight averages. Increasing the CTA concentration 2-fold significantly decreased the molecular weight averages due to the chain transfer reaction. Comparison between runs MV1 and MV3 indicates that increases in initiator concentration contributed to slightly higher molecular weight averages. This agreed with the increasing polymerization reaction rate as shown previously in Figs. 10 and 12. Combined effects of increases in initiator concentration and decreases in CTA concentration on the molecular weight averages were also observed. Though

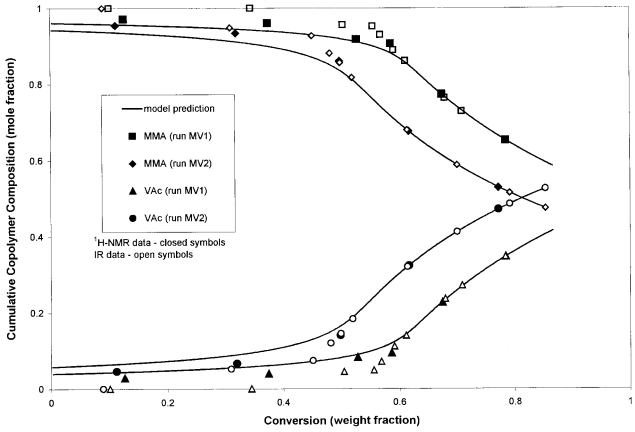

Fig. 14. MMA/VAc solution copolymerization runs MV1 and MV2: cumulative copolymer composition vs. conversion.

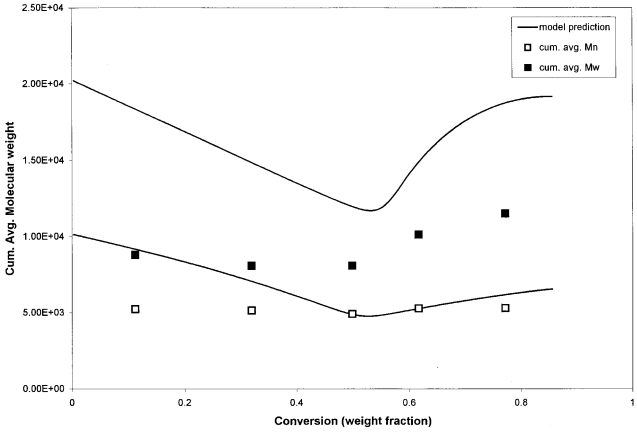

Fig. 16. MMA/VAc solution copolymerization run MV2: cumulative number- and weight-average molecular weight vs. conversion.

increases in initiator concentration resulted in slightly higher molecular weight averages, higher CTA concentrations led to lower molecular weight averages and narrower molecular weight distributions.

Solvent effects on VAc rate coefficients can be significant because toluene, like other aromatic solvents, acts as a strong retardant for VAc homopolymerization [28]. Radical–solvent complexes may lead to the stabilization of unstable VAc radical intermediates. The modified lumped parameter used to incorporate the solvent effect, based on a chain length dependence for k_t, for VAc polymerization modelling was introduced from similar modelling efforts for BA/VAc solution copolymerizations in toluene [32]. Model predictions for overall conversions, copolymer compositions, and molecular weight averages for the most part, are reasonably good (see Figs. 12–16). There are some discrepancies between model predictions of VAc conversion and experimental data at high overall conversions. These model predictions were achieved using the homopolymerization parameters for each system directly. Efforts are currently underway to improve the model predictions by investigating alternative models and improving parameter estimates in the light of the effects of solvent and CTA for the prediction of molecular weight averages and molecular weight distributions.

4. Conclusions

The results obtained from off-line monitoring of BA, MMA, and VAc solution homo- and copolymerizations showed that ATR-FTIR spectroscopy is well suited for polymerization reaction monitoring and kinetic investigations. The data acquired through ATR-FTIR spectroscopy showed good agreement with data from conventional gravimetric and ^{1}H-NMR analysis.

A great deal of information on the characteristic absorbances of the monomers in this study was collected. This information can be used for further application of the ReactIR™ 1000 ATR-FTIR probe to the study to in-line solution and emulsion polymerization monitoring.

The incorporation of solvent effects on model parameters for BA and VAc resulted in improved predictions on conversion, copolymer composition and molecular weight averages. Predictions of MMA and BA/MMA solution polymerizations were in good agreement with the experimental results. Improvements to the model predictions for the MMA/VAc system at high conversion are the subject of future work.

These findings should have an impact on our ability to implement improved process control strategies on polymer systems that exhibit large composition drift.

Acknowledgements

The authors wish to gratefully acknowledge financial support from the Natural Science and Engineering Research Council (NSERC) of Canada, the Canada Foundation for Innovation (CFI), and the Province of Ontario Research and Development Challenge Fund.

References

[1] Kammona G, Chatzi EG, Kiparissides C. J Macromol Sci — Rev Macromol Chem Phys 1999;C39:57–134.
[2] Chien DCH, Penlidis A. J Macromol Sci — Rev Macromol Chem Phys 1990;C30:1–42.
[3] Dallin P. Process Control Qual 1997;9(4):167–72.
[4] Koenig JL. Spectroscopy of polymers. 2nd ed. New York: Elsevier Science, 1999.
[5] Mijovic J, Andjelic S. Polymer 1996;37(8):1295–303.
[6] Doyle WM. Process Control Qual 1992;2:11–41.
[7] Puskas JE, Lanzendörfer MG, Pattern WE. Polym Bull 1998;40:55–61.
[8] Puskas JE, Lanzendörfer MG. Macromolecules 1998;31:8684–90.
[9] Storey RF, Donnalley AB, Maggio TL. Macromolecules 1998;31:1523–6.
[10] Storey RF, Donnalley AB. Macromolecules 1999;32:7003–11.
[11] Storey RF, Maggio TL. Macromolecules 2000;33:681–8.
[12] Pasquale AJ, Long TE. Macromolecules 1999;32:7954–7.
[13] Dubé MA, Penlidis A. Polymer 1995;36(3):587–98.
[14] Dubé MA, Penlidis A. Macromol Chem Phys 1995;196:1101–12.
[15] Dubé MA, Penlidis A. Polym Int 1995;37:235–48.
[16] Choi KY, Butala DN. Polym Engng Sci 1991;31(5):353–64.
[17] Noël LFJ, Brouwer ECP, van Herk AM, German AL. J Appl Polym Sci 1995;57:245–54.
[18] http://www.ampolymer.com/mark-%20houwink%20parameters.htm.
[19] McKenna TF, Villanueva A, Santos AM. J Polym Sci A: Polym Chem 1999;37:571–88.
[20] Brandrup J, Immergut EH, editors. Polymer handbook. New York: Wiley, 1989.
[21] Chatzi EG, Kammona O. J Appl Polym Sci 1997;63:799–809.
[22] Smith B. Fundamentals of Fourier transform infrared spectroscopy. Boca Raton: CRC Press, 1996.
[23] Badeen C. MASc thesis, Department of Chemical Engineering, University of Ottawa, Ottawa, 2000.
[24] Dubé MA, Soares JBP, Penlidis A, Hamielec AE. Ind Engng Chem Res 1997;36:966–1015.
[25] Gao J, Penlidis A. J Macromol Sci — Rev Macromol Chem Phys 1996;C36:199–404.
[26] Gao J, Penlidis A. J Macromol Sci — Rev Macromol Chem Phys 1998;C38:653–781.
[27] Fernandez-Garcia M, Martinez JJ, Madruga EL. Polymer 1998;39(4):991–5.
[28] Coote ML, Davis TP, Klumperman B, Monteiro MJ. J Macromol Sci — Rev Macromol Chem Phys 1998;C39:567–636.
[29] McManus NT, Dubé MA, Penlidis A. Polym React Engng 1999;7(1):131–45.
[30] Hakim M, Verhoeven V, McManus NT, Dubé MA, Penlidis A. J Appl Polym Sci 2000;77(3):602–9.
[31] Madruga EL, Fernandez-Garcia M. Macromol Chem Phys 1996;197:3743–55.
[32] Jovanovic R, Dubé MA. Off-line monitoring of butyl acrylate and vinyl acetate homo- and copolymerization in toluene. Submitted for publication.
[33] Scorah MJ, Hua H, Dubé MA. Bulk and solution copolymerization of methyl methacrylate and vinyl acetate. J Appl Polym Sci 2001 (in press).